

Effect of K_2SO_4 on solvent extraction of vanadium with D2EHPA/TBP

Nan-nan Xue^{a,b}, Yi-min Zhang^{a,b,c,*}, Tao Liu^{a,b,c}, Jing Huang^{a,b,c}, Hong Liu^{a,c}

^a School of Resource and Environmental Engineering, Wuhan University of Science and Technology, Wuhan 430081, China

^b Hubei Provincial Engineering Technology Research Centre of High Efficient Cleaning Utilization for Shale Vanadium Resource, Wuhan 430081, China

^c Hubei Collaborative Innovation Centre for High Efficient Utilization of Vanadium Resources, Wuhan 430081, China

*Corresponding author, e-mail: zym126135@126.com

Received 3 Aug 2017

Accepted 29 Sep 2017

ABSTRACT: The effect of K_2SO_4 on the vanadium extraction with bis(2-ethylhexyl) phosphoric acid (D2EHPA)/tributyl phosphate (TBP) was studied in a pressure acid leaching system of stone coal. K_2SO_4 intervention achieved good removal of Al and Fe on the premise of high V leaching efficiency during pressure acid leaching. Studies show that when the K_2SO_4 dosage is 7 wt.%, the H_2SO_4 concentration is 15 vol.%, the liquid/solid ratio is 1.5 ml/g, the leaching temperature is 190 °C, and the leaching time is 5 h, then 90% of V can be leached, but only 30% of Al and 6% of Fe are leached together. After four-stage countercurrent extraction with 20% vol D2EHPA at pH 1.8, the loaded organic phase showed a feature of more V ions with fewer Al and Fe ions, indicating that K_2SO_4 intervention reduced the impurity load of vanadium extraction from stone coal acid leaching solution.

KEYWORDS: stone coal, pressure acid leaching, vanadium extraction

INTRODUCTION

With the increasing market demand for vanadium products and the shortage of high-grade ores, it becomes increasingly necessary and urgent to exploit and utilize stone-coal resources for vanadium pentoxide production¹. The stone coal is an important vanadium-bearing resource, which is widely distributed in many provinces of China^{2,3}. In stone coal, the vanadium exists mostly as trivalent vanadium (V(III)); tetravalent and pentavalent vanadium are very scarce⁴⁻⁷. V(III) replaces Al(III) isomorphically in muscovite lattice, which means that vanadium in stone coal is difficult to extract.

The conventional process flow of vanadium recovery from stone coal includes roasting, acid leaching, purification, precipitation, and calcination. The muscovite structure is stable, so roasting and leaching are the most effective methods of breaking down the lattice structure of muscovite. In recent years, oxygen acid leaching of stone coal has drawn increasing attention due to more serious air pollution and higher energy consumption caused by roasting. The pressure acid leaching strengthens the leaching

of V via the increase of leaching temperature under pressure field instead of addition of fluoride in forms such as HF, ammonium fluoride or fluorite, or oxidant in forms such as sodium hypochlorite or MnO_2 ⁸. However, the two leaching methods are associated with a difficulty in separating V from impurities Al and Fe.

When the leaching solution contains massive impurities, the purification of the acid leaching solution naturally turns into another difficulty. Solvent extraction⁹⁻¹¹ and ion exchange^{12,13} are the two most frequently used methods to obtain a concentrated vanadium solution. The ion exchange process is cost-effective and easy to operate, and various types of resins have been reported to recover vanadium from a neutral solution¹⁴, alkaline solution¹⁵, or acid solution¹⁶. However, ion exchange is more often applied to extract V(V) from low acid solutions with low concentrations of impurities. Solvent extraction is more widely used because of its high selectivity, fast reaction rate, and high recovery of metal ions. It has also been employed in commercially extractive metallurgy.

Currently, various extractants have been used

to recover vanadium from acid solutions: bis(2-ethylhexyl) phosphoric acid (D2EHPA)¹⁷, 2-ethylhexyl phosphonic acid mono-2-ethyl hexyl ester (EHEHPA)¹⁸, 5,8-diethyl-7-hydroxydodecane-6-oxime (LIX 63)¹⁹, dithiophosphinic acid (Cyanex)²⁰, and trialkylamine (Alamine 336)²¹, of which D2EHPA has been widely used due to its economic cost, acidic adaptability, excellent extraction selectivity, and high extraction efficiency. Some studies have been conducted to investigate effects of metal ions on solvent extraction of V(IV) by D2EHPA, concluding that this extractant presents excellent selectivity to V(IV) over K, Na, and Mg ions but weak selectivity over Al and Fe ions in the acid leaching solution of stone coal²². Thus the stages of vanadium extraction with D2EHPA will be long because of co-extractions of massive Al and Fe ions, which increases the impurity load of vanadium extraction prolonging the production recycle. If Al and Fe ions were separated with V in a leaching process, Al and Fe ions would be limited to access to the extraction process. After stripping, the vanadium-enriched solution with few impurities would be easier to obtain. The less impurities in the vanadium-enriched solution, the higher the purity of V₂O₅ product will be.

This work, therefore, investigates the effect of K₂SO₄ intervention on leaching and extraction of vanadium, aiming at reducing the impurity load of vanadium extraction via K₂SO₄ intervention. Then a flow sheet for the selective separation and recovery of vanadium from stone coal was designed to remove Al and Fe from sources and to lower the impurity load.

MATERIALS AND METHODS

Materials and apparatus

The stone coal used in the study was obtained from Hubei province, South China. Various chemical reagents, including H₂SO₄, K₂SO₄, Ca(OH)₂, D2EHPA, TBP, sulphonated kerosene, NH₄OH, and NaClO₃ were used during the whole process.

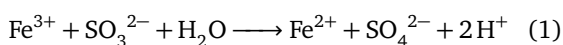
Chemical compositions of stone coal and the aqueous solution were measured using inductively coupled plasma-atomic emission spectrometry (ICP-AES, IRIS Advantage Radial, USA). The mineralogical composition of the stone coal was identified by X-ray diffractometer with Cu K α radiation (XRD, Bruker D8 Advance, Germany). The surface morphology of the raw stone coal and the corresponding EDS analysis were examined using a scanning electron microscope with energy dis-

perse spectroscopy (SEM, JSM-6610, Jeol, Japan; EDS, XT2000, Oxford, UK). The pore analysis of the leaching residues was investigated by specific surface area and porosity analyser (ASAP 2000, Micromeritics, USA). The vanadium valence of raw stone coal and leaching solution were determined by the potentiometric titration method²³. The solution pH measurement was performed with a pH meter (Mettler Toledo S220, Greifensee, Switzerland).

Experiments

The leaching experiments were carried out in a pure zirconium reaction kettle with a volume of 2 l and conducted by a programmable temperature controller with a deviation of ± 3 °C. The test samples are obtained after being crushed and ground to a state in which minus 0.074 mm accounts for more than 85% of the sample. The test sample, K₂SO₄ powder (added in terms of mass ratio), and the prepared H₂SO₄ solution were loaded into the reaction kettle and mixed adequately through mechanical stirring at 350 rpm. The used oxygen in the experiments, from an oxygen cylinder, was introduced into the reaction kettle when the temperature reached the set value. The purity of oxygen was 98%. After reaction, the leaching residues and leaching solution were obtained through solid-liquid separation.

The Fe(III) and V(V) in the leaching solution were firstly reduced to Fe(II) and V(IV) with 1.5 times the theoretical amount of Na₂SO₃ because D2EHPA, used as extractant, was in favour of extracting V(IV) than V(V) and Fe(III) than Fe(II)²⁴:



Then the pH value of the leaching solution was adjusted by 400 g/l Ca(OH)₂ emulsion. The feed solution was thus obtained for the solvent extraction. The extraction experiments were performed in a glass reactor at room temperature with stirring speed of 500 rpm by mixing the aqueous phase with the organic phase containing D2EHPA as extractant and tri-butyl phosphate (TBP) as phase modifier. The mixtures were separated in a separating funnel, which yielded the loaded organic phase and the raffinate. An 8 vol.% H₂SO₄ solution was used as the stripping agent. The stripping experiments were also carried out in a glass reactor with 1.6 mol/l H₂SO₄ solution as stripping agent, O/A ratio of 5, contacting time of 20 min. After mixing, the stripping solution and the unloaded organic phase were obtained.

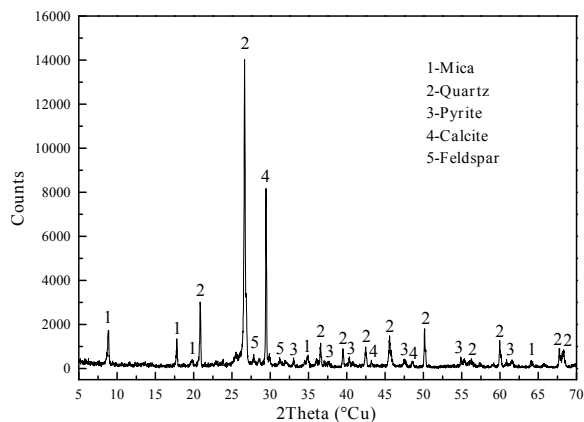


Fig. 1 The XRD pattern of the stone coal.

RESULTS AND DISCUSSION

Characterization of raw stone coal

The V_2O_5 grade was 0.76% of total mass and Si, Al, Fe, Ca, K, Na, Mg, C, P accounted for 23%, 4.8%, 3.5%, 4.3%, 2.5%, 0.65%, 1.2%, 11%, and 0.23% of total mass, respectively. The XRD pattern of the stone coal is shown in Fig. 1. The major minerals in stone coal were quartz, muscovite/illite, calcite, pyrite, and feldspar. Then, the chemical phases of vanadium in stone coal were analysed by gradient elution analysis²⁵, with the results that 81% V was distributed in alumino-silicate minerals, 15% V in organic matter, and 5% V in free oxide.

The chemical constituents of the major minerals in stone coal are shown in Table 1 obtained by EDS analysis. The vanadium mainly exists in the crystal lattice of muscovite or illite where V(III) isomorphically replaces Al(III). Fe exists in pyrite, muscovite, and illite while Al exists in muscovite and illite. So Al ions come from the dissolution of muscovite and illite. Fe/S molar ratio was calculated to be 0.55, from which it was deduced that Fe mostly exists in pyrite. So Fe ions come from pyrite dissolution. Fig. 2 showed the SEM patterns of the morphology of muscovite in raw stone coal. It is clearly seen that there are a number of projections and con-

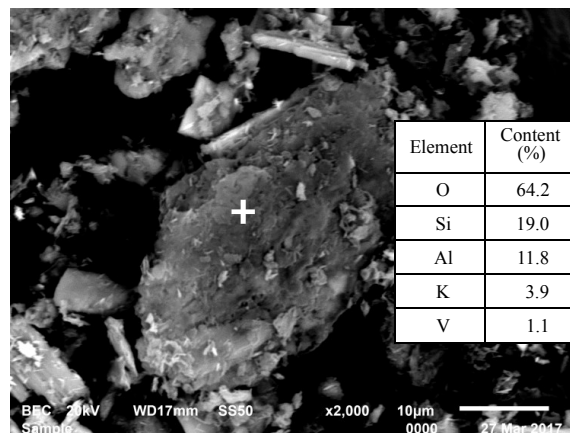


Fig. 2 SEM patterns of vanadium-containing minerals in raw stone coal.

cave corners appearing on muscovite surfaces before leaching, but the muscovite particles still retain a compact surface.

Effect of K_2SO_4 on vanadium leaching

K_2SO_4 can stimulate $CaSO_4$ hydration to become $CaSO_4 \cdot 2H_2O$ below 100 °C; $CaSO_4 \cdot 2H_2O$ then dissolves and recrystallizes in the form of $CaSO_4$ over 100 °C^{26,27}. The transition of $CaSO_4 \cdot 2H_2O \rightarrow CaSO_4$ improves the crystallinity of $CaSO_4$ crystals, increasing their strength and toughness²⁸. The nucleation rate shows a nonlinear dependence on the prevailing, activity-based supersaturation²⁹. When stone-coal reacts with H_2SO_4 , K_2SO_4 , Na_2SO_4 and other species are slowly generated with $CaSO_4$ from calcite dissolution. So the instantaneous supersaturation of $CaSO_4 \cdot 2H_2O$ is very low. If K_2SO_4 is added from the beginning of pressure acid leaching, the high instantaneous supersaturation of $CaSO_4 \cdot 2H_2O$ accelerates the formation of $CaSO_4 \cdot 2H_2O$ instead of $CaSO_4$, because of the high SO_4^{2-} concentration induced by K_2SO_4 produced a common-ion effect significantly decreasing the solubility of $CaSO_4 \cdot 2H_2O$ ²⁷. Meanwhile, as a result of lower nucleation energy from concave corners

Table 1 Main chemical compositions of the major minerals in stone coal (at %).

Mineral	V_2O_3	O	Si	Al	Fe	Mg	Ca	Na	K_2O	S	C
Pyrite			0.03		45.98					54.98	
Calcite		58.74				0.66	19.90				20.70
Quartz		54.04	45.96								
Muscovite	2.37	39.04	23.87	14.41	0.18	2.72	0.01	0.05	7.90		9.45
Illite	2.82	51.43	18.67	12.30	0.11	1.21	0.11	0.06	7.09		6.20

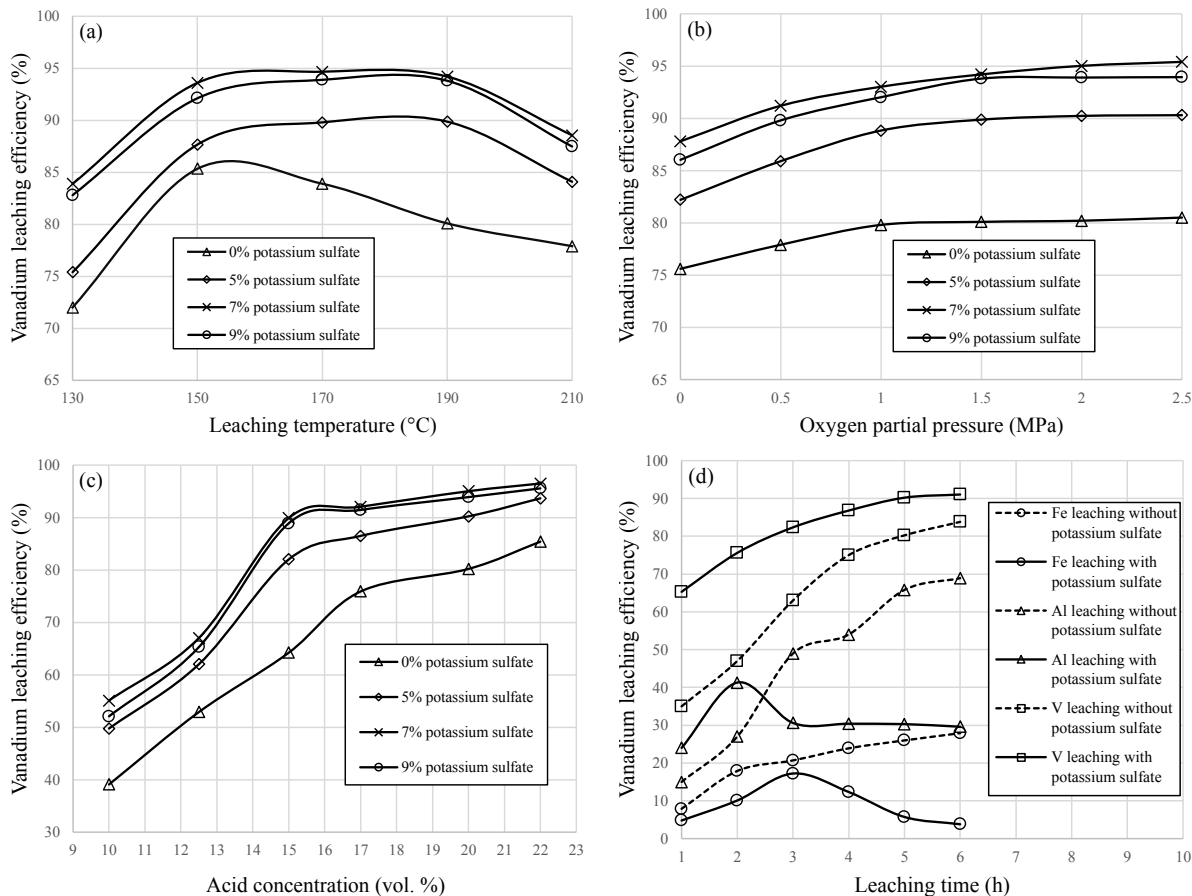


Fig. 3 Effect of leaching parameters on leaching efficiency with K_2SO_4 assistance. (a) Effect of leaching temperature on vanadium leaching efficiency at different K_2SO_4 dosages; (b) effect of oxygen partial pressure on vanadium leaching efficiency at different K_2SO_4 dosages; (c) effect of sulphuric acid concentration on vanadium leaching efficiency at different K_2SO_4 dosages; (d) effect of leaching time on leaching efficiencies of V, Al, and Fe with and without K_2SO_4 assistance.

and projections of substrate materials other than from aqueous solution²⁹, $CaSO_4$ can recrystallize on stone coal particles over 100 °C.

Hence basing on the above transition phenomena, a series of experiments were carried out to determine the optimum leaching conditions under K_2SO_4 assistance and the influences of operating parameters on leaching efficiency (Fig. 3).

With K_2SO_4 dosage change, the effect of leaching temperature on vanadium leaching efficiency under conditions of acid concentration of 20 vol.%, oxygen partial pressure of 1.5 MPa and leaching time of 5 h is presented in Fig. 3a. The vanadium leaching efficiency under K_2SO_4 assistance was higher than that with no assistance. It increased quickly and then levelled off below 190 °C; when the leaching temperature exceeded 190 °C, the vanadium leaching efficiency started to decrease. At

190 °C, about 95% vanadium was leached using over 7 wt.% K_2SO_4 . Hence the optimal leaching temperature was set to 190 °C.

The effect of O_2 partial pressure on vanadium leaching efficiency under conditions of acid concentration of 20 vol.%, 190 °C, and leaching time of 5 h is shown in Fig. 3b. Under 7 wt.% K_2SO_4 assistance, the vanadium leaching efficiency went up from 88% to 95% below 2.0 MPa oxygen partial pressure and then levelled off. According to the results presented by Heduit³⁰, the oxygen solubility increases directly with oxygen partial pressure and slightly with increased temperature. Increasing oxygen partial pressure favour the leaching of V(III) ions because oxygen is the main oxidizing reagent in the leaching of stone coal. Under 2.0 MPa oxygen partial pressure, about 95% vanadium was leached using over 7 wt.% K_2SO_4 . The optimal oxygen

partial pressure was set to 2.0 MPa.

The effect of acid concentration on vanadium leaching efficiency under conditions of 190 °C, 2.0 MPa oxygen partial pressure, and leaching time of 5 h is shown in Fig. 3c. As the acid concentration was less than 15 vol.%, the vanadium leaching efficiency increased quickly under K_2SO_4 assistance; with a further increase of acid concentration from 15 vol.% to 22 vol.%, the increase of vanadium leaching efficiency slowed down. In 15 vol.% H_2SO_4 solution, about 90% vanadium was leached using over 7 wt.% K_2SO_4 . Hence the optimal acid concentration was set to 15 vol.%.

The effect of leaching time on leaching efficiency of Al, Fe, and V with and without K_2SO_4 assistance is presented in Fig. 3d under the above-mentioned optimum leaching conditions. The aluminium leaching efficiency firstly increased during two hours and then descended to a stable value (31%) in one hour under K_2SO_4 assistance. However, the aluminium leaching efficiency increased all the time under no assistance. The iron leaching efficiency under K_2SO_4 assistance firstly increased during three hours and then descended to the stable value (6%) in the next two hours. But the iron leaching efficiency with no assistance kept increasing over time. Hence K_2SO_4 addition derived the decreases of leaching efficiencies of Al and Fe. When leaching for 5 h, the leaching efficiency of V, Al, and Fe achieved 90%, 30%, and 6%, respectively, marking an effective separation of V ions over Al and Fe ions.

The XRD results of leaching residues are presented in Fig. 4. At 80 °C, the mineral phases were quartz, muscovite, feldspar, pyrite, and gypsum. When the leaching temperature exceeded 100 °C, the mineral phases clearly changed. At 150 °C, the mineral phases became quartz, muscovite, feldspar, and anhydrite. At 190 °C, the mineral phases became quartz, feldspar, anhydrite, alunite ($KAl_3(SO_4)_2(OH)_6$), and yavapaiite ($KFe(SO_4)_2$). Gypsum was transformed into anhydrite and the alunite and yavapaiite formed with the increasing of leaching temperature, indicating progress of the transition from $CaSO_4 \cdot 2H_2O$ to $CaSO_4$ and of precipitation of Al and Fe ions. Thus the leaching of Al and Fe from muscovite and pyrite was concomitant with the precipitation of the leached Al and Fe ions at 190 °C, decreasing the leaching efficiencies of Al and Fe (Fig. 3d). Meanwhile, the leached V ions can stably exist in aqueous solution. It was concluded that the effective separations of Al and Fe ions were due to the formation of $KAl_3(SO_4)_2(OH)_6$ and

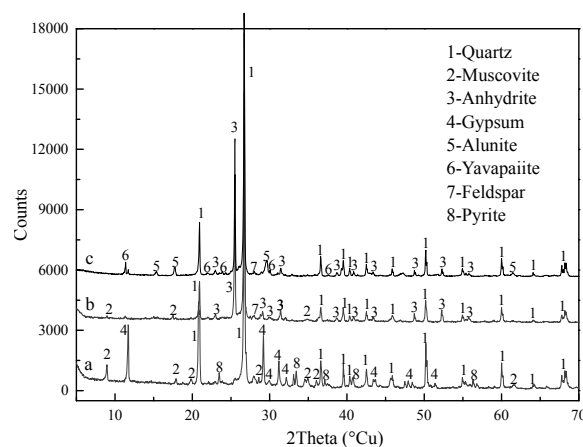


Fig. 4 XRD pattern of leaching residues after leaching for 5 h with 20 vol.% H_2SO_4 solution, 2.0 MPa oxygen partial pressure and 7 wt.% K_2SO_4 at (a) 80 °C, (b) 150 °C, and (c) 190 °C.

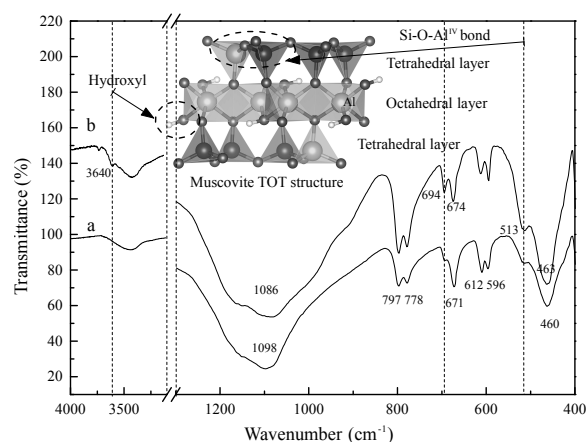


Fig. 5 FTIR spectra of leaching residues after leaching at 190 °C: (a) with K_2SO_4 assistance; (b) no assistance.

$KFe(SO_4)_2$ in K^+ -rich solution environment created by K_2SO_4 addition.

The bonding structures of leaching residues with and without K_2SO_4 assistance were compared by FTIR analysis (Fig. 5). In muscovite structure, Al_2OH vibration was located at 3604 cm^{-1} ; the strong band at 694 cm^{-1} is related to $Al^{IV}-O$ stretching vibration within the tetrahedron layer; the weak band at 513 cm^{-1} belongs to $Al^{IV}-O$ bending vibration vertical to the tetrahedron layer³¹. At acidic pH, the dissolution rate of muscovite tended to be controlled by the breaking of $Si^{IV}-O$ bonds after adjoining Al^{IV} has been removed by a proton exchange reaction³². But owing to incongruous dissolution of muscovite, Si was unable to dissolve. Thus the

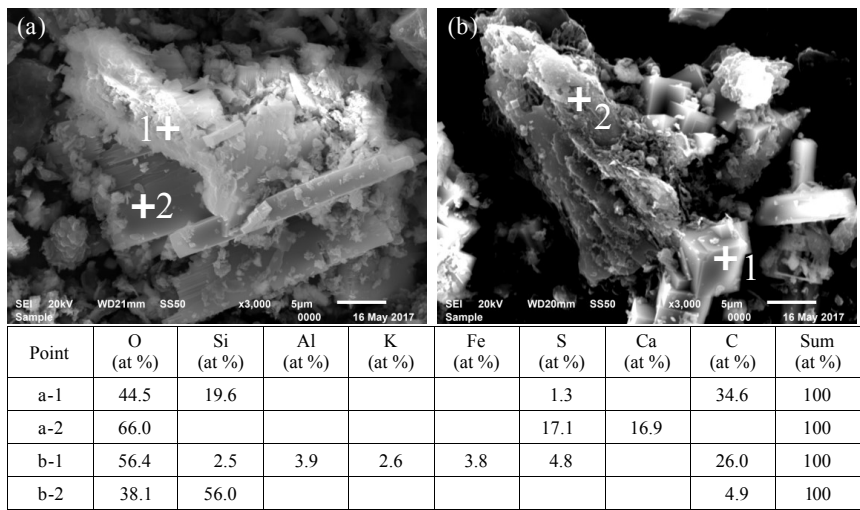


Fig. 6 SEM-EDS patterns of leaching residues under K_2SO_4 assistance at $190\text{ }^\circ\text{C}$.

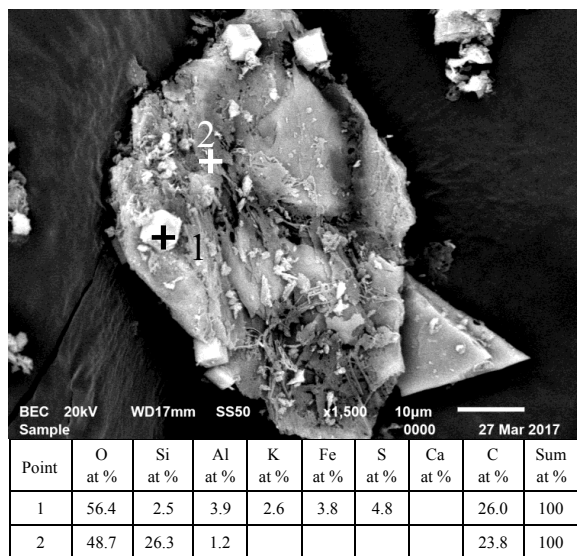


Fig. 7 SEM-EDS patterns of leaching residues under no assistance at $190\text{ }^\circ\text{C}$.

dissolution rate of muscovite should be decided by the breaking of $Al^{IV}-O$ bond. In contrast, the bands at 3604 cm^{-1} , 694 cm^{-1} , and 513 cm^{-1} disappeared under K_2SO_4 assistance and showed up under no assistance, indicating that Al^{IV} in the tetrahedron and hydroxyl in the octahedron no longer existed under K_2SO_4 assistance. K_2SO_4 assistance thus completely dissolved the Al atoms from the muscovite lattice.

The morphologies of leaching residues with and without K_2SO_4 assistance are shown in Fig. 6 and Fig. 7. An obvious interface bonding occurred between $CaSO_4$ crystals and dissolve debris of mus-

covite, which was judged according to the corresponding EDS results in Fig. 6. The alunite crystals, as aggregations, were also embedded deeply in the dissolved debris of muscovite. Only isolated alunite crystals grew on muscovite particle surface under no assistance, but the muscovite particle surface was broken weakly (Fig. 7). Hence, comparing the surface feature of muscovite in Fig. 2, $CaSO_4$ and alunite crystals grew up in muscovite particles and the muscovite particles were cracked and etched more seriously under K_2SO_4 assistance.

During the acid leaching of stone coal, V was released from the interfaces between muscovite and H_2SO_4 solution. Hence considering the morphological features and bonding structure of muscovite, $CaSO_4$, and alunite crystals act on the muscovite matrix, causing the muscovite particles crack. This behaviour increased the reactive interfaces and finally enhanced the release of vanadium.

Effect of K_2SO_4 on vanadium extraction from acid leaching solution

The acid leaching solution (K-1) was obtained after leaching under the above-mentioned optimum leaching conditions. The concentrations of aluminium and iron ions in solution K-1 are far below the concentration levels in the acid leaching solution obtained by leaching without K_2SO_4 addition (B-1) (Table 2). A series of experiments were performed to determine the optimum extraction conditions of K-1 and the influences of operating parameters on the extraction efficiency are presented in Fig. 7.

The effects of the initial pH value on the extraction of vanadium and impurity ions are shown

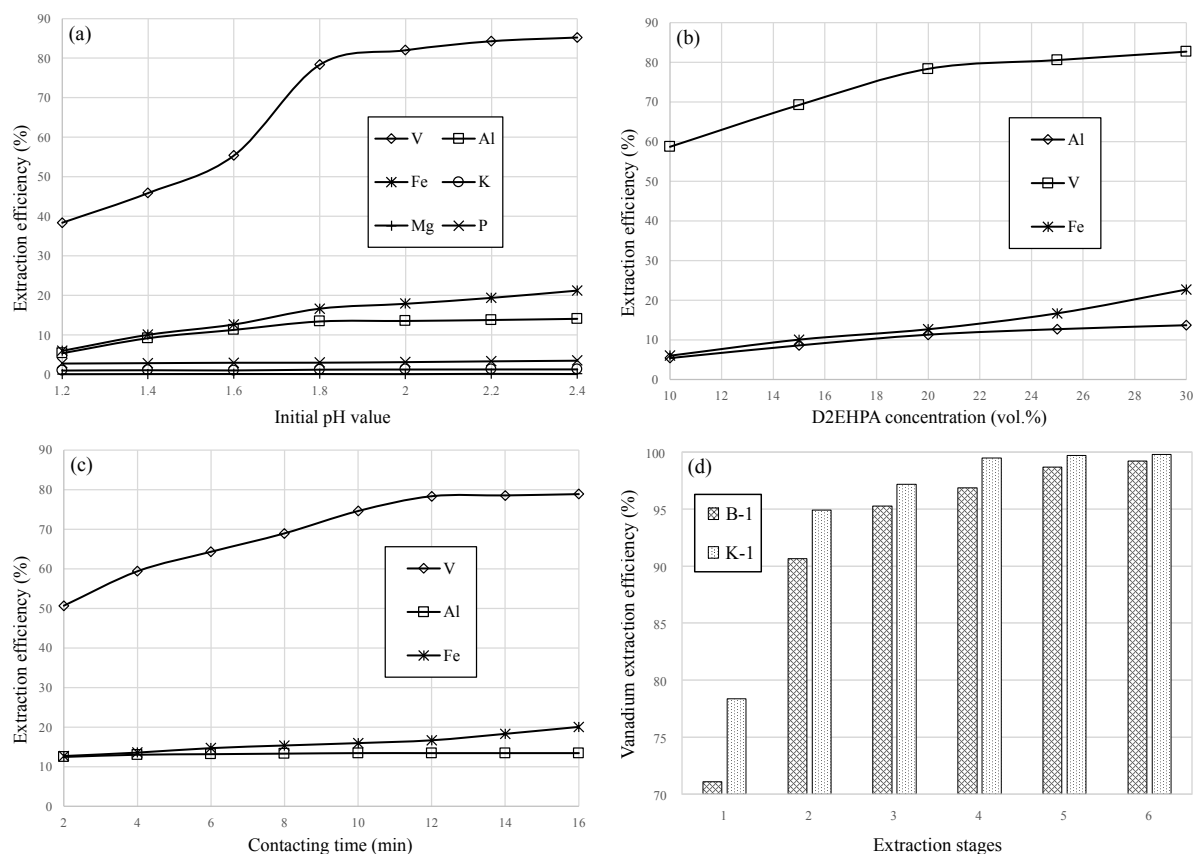


Fig. 8 Effects of extraction conditions on the extraction efficiencies of vanadium and impurity ions. (a) Effect of initial pH value; (b) effect of D2EHPA concentration; (c) effect of contacting time; (d) effect of extraction stage on vanadium extraction.

Table 2 Composition of the acid leaching solution (g/l).

ALS [†]	V	Al	Fe	K	Mg	Na	P
K-1	1.81	7.49	0.98	3.47	3.46	3.75	1.14
B-1	1.79	13.88	5.09	3.81	3.72	2.02	0.51

[†] Acid leaching solution.

in Fig. 8a with an organic phase composition of 20 vol.% D2EHPA and 5 vol.% TBP, A/O phase ratio of 2, and extraction time of 12 min. The results show that vanadium extraction was sensitive to the initial pH value as the extraction efficiency rapidly increased from 38% to 78% when the pH increased from 0.0–1.8. On the other hand, impurity ions showed different variation trends in the extraction efficiency. The extraction efficiencies of Al and Fe increased from 5% to 13% and 6% to 17%, respectively, with the pH changed while the extraction of P, Mg, K, and Na was almost null. Thus Fe and Al ions had adverse impacts on vanadium extraction. Nevertheless, when the initial pH was higher than

1.8, the vanadium extraction levelled off and the iron extraction increased further. Hence the optimal solution pH was determined to be 1.8.

Under the conditions of initial pH of 1.8, A/O phase ratio of 2, and contacting time of 12 min, the effects of D2EHPA concentration on extraction of V, Fe, and Al were performed, (Fig. 8b). The vanadium extraction efficiency increased from 59% to 79% as the D2EHPA concentration in the organic phase increased from 5 vol.% to 20 vol.%, which indicated that the D2EHPA concentration also influenced vanadium extraction greatly. However, with the increase of D2EHPA concentration from 20 vol.% to 30 vol.%, the extraction of vanadium increased only 4% while the aluminium extraction levelled off and the iron extraction increased further. Additionally, the viscosity of the organic phase increased because of high extractant concentration, making it difficult for the organic phase to be mixed with aqueous solutions and time-consuming to reach equilibrium. Hence the optimum D2EHPA concentration was chosen as 20 vol.%.

To determine the effects of contacting time on extraction of V, Fe, and Al, the experiments were performed under the conditions of initial pH of 1.8, A/O phase ratio of 2, and D2EHPA concentration of 20 vol.%. Fig. 8c showed that as the contacting time increased, vanadium extraction firstly increased and then tended to be stable. Furthermore, the iron extraction gradually increased and the aluminium extraction was almost constant with the contacting time increasing. Hence the optimum contacting time was chosen as 12 min.

The effects of extraction stage on vanadium extraction from K-1 and B-1 at the above-mentioned optimal extraction conditions were also investigated (Fig. 8d). At one-stage extraction, 72% of vanadium in B-1 and 78% of vanadium in K-1 were extracted, indicating that vanadium extraction accelerated after K_2SO_4 intervention. After four-stage extractions, the vanadium extraction of K-1 reached 99.2%. The vanadium extraction of B-1, however, needed six-stage extractions to reach 99.5%. High Al and Fe concentrations lead to an increase in extraction stages because of the co-extraction. Thus V ions reached an extraction equilibrium quickly because of less Al and Fe contents in acid leaching solution after K_2SO_4 intervention.

Then, the four-stage countercurrent extraction of K-1 was carried out, with the results that the extraction efficiencies of V, Al, and Fe reached 98%, 12% and 13%, respectively, after four-stage counter-flow solvent extraction. The raffinate was collected and analysed (Table 3). According to the results of leaching efficiency and extraction efficiency of V, Al, and Fe under the optimal leaching and extraction conditions, the distribution ratios of V, Al, and Fe in loaded organic phases were calculated (Table 4). The loaded organic phase from K-1 showed a feature of more V ions with fewer Al and Fe ions. Hence the impurity load of vanadium extraction was reduced after K_2SO_4 intervention.

The loaded organic phases were stripped using H_2SO_4 solution as stripping agent. The results showed that when stripping agent was 1.6 mol/l H_2SO_4 solution, O/A ratio was 5, and contacting

Table 3 Elemental concentrations in raffinate and stripping solution (g/l).

De ^a	V	Al	Fe	K	Mg	Na	P
R ^b	0.028	6.356	0.750	3.082	3.435	5.818	1.103
Ss ^c	14.965	0.944	0.091	0.015	0.011	0.023	0.030

^a Dissolved elements; ^b Raffinate; ^c Stripping solution

Table 4 The distribution ratios of V, Al, and Fe in loaded organic phase (wt.%).

Loaded organic phase	V	Al	Fe
From K-1	88.7	3.6	0.7
From B-1	78.8	6.6	3.6

time was 20 min, the stripping yields of V, Al, and Fe reached 99.50%, 13% and 17%, respectively, after three-stage counter-flow anti-extraction. The main chemical compositions of the stripping solution are listed in Table 3. The stripping solution contained 14.97 g/l V, 0.944 g/l Al, and 0.091 g/l Fe, respectively.

Precipitation of V_2O_5

The V_2O_5 product was obtained after oxidation, ammonium salt precipitation, and calcination. Firstly, $NaClO_3$ was added in the stripped solution to oxidize VO^{2+} to VO_2^+ . Then NH_4OH was added into the stripped solution to adjust pH value to 1.8 and then precipitate ammonium metavanadate at 95 °C for 1 h. The precipitate was filtered and dried before being roasted in a muffle furnace at 500 °C for 1 h to obtain V_2O_5 . The chemical compositions of the V_2O_5 product are presented in Table 5. The purity of V_2O_5 product reached 99% with trace impurities, meeting the Related Chinese Industry Standards (YB/T5304-2011). The high-quality V_2O_5 can be prepared finally.

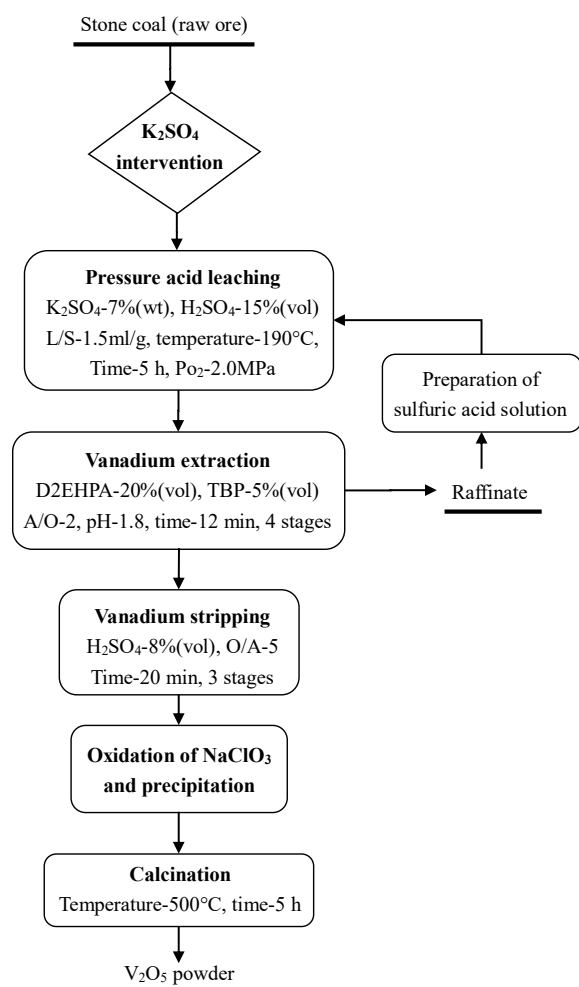
Process flow sheet for vanadium recovery from stone coal

Based on the above studies, a flow sheet of vanadium recovery from stone coal was established (Fig. 9). The V_2O_5 product can be prepared through K_2SO_4 -assisted pressure acid leaching, solvent extraction (D2EHPA-TBP-sulphonated kerosene), stripping with H_2SO_4 solution, precipitation, and calcination. At first, via leaching under conditions of K_2SO_4 dosage of 7 wt.%, H_2SO_4 concentration of 20 vol.%, liquid-to-solid ratio of 1.5 ml/g, leaching temperature of 190 °C, O_2 partial pressure of 2.0 MPa, and leaching time of 5 h, the acid leaching solution can be obtained. Then, through four-stage countercurrent extraction and three-stage countercurrent stripping, the stripping solution with few impurities can be obtained. After $NaClO_3$ oxidation, V(IV) ions in the stripping solution are reduced to be V(V) ions and crystallized as ammonium metavanadate at 95 °C and pH value of 1.8 with the addition of ammonia. The

Table 5 Chemical compositions of V_2O_5 product.

Product	Composition (%)						
	V_2O_5	Si	P	S	Fe	As	$K_2O + Na_2O$
V_2O_5 product in this study	98.98	0.14	0.02	0.01	0.25	null	0.06
YB/T5304-2011 V_2O_5 98	98.00	0.25	0.05	0.03	0.30	0.02	1.50

V_2O_5 product with a purity more than 98% can be obtained after roasting at 550 °C for 1 h. The raffinate returns to the pressure acid leaching step after being used to prepare H_2SO_4 solution. The cycle utilization of raffinate reduces K_2SO_4 wastage because the raffinate contains a lot of K ions. The vanadium recovery of the whole process was 88%.

**Fig. 9** All-wet enhanced process of vanadium recovery from stone coal.

CONCLUSIONS

The removal of Al and Fe was coupled with the leaching of V under K_2SO_4 intervention during pressure acid leaching. The effective separations of Al and Fe ions were due to the formation of $KAl_3(SO_4)_2(OH)_6$ and $KFe(SO_4)_2$ in K^+ -rich solution environment created by K_2SO_4 addition.

With 7 wt.% K_2SO_4 dosage, 15 vol.% H_2SO_4 , liquid/solid ratio of 1.5 ml/g, leaching temperature of 190 °C, and 5 h leaching time, 90% of V could be leached, but only 30% of Al and 6% of Fe were leached together. After a four-stage countercurrent extraction with 20 vol.% D2EHPA and 5 vol.% TBP at pH 1.8, the loaded organic phase showed a feature of more V ions with fewer Al and Fe ions. V ions reached an extraction equilibrium quickly because of less Al and Fe contents in acid leaching solution after the K_2SO_4 intervention.

A flow sheet for the selective separation and recovery of vanadium from stone coal was developed via the combinations of K_2SO_4 -assisted pressure acid leaching, solvent extraction by D2EHPA/TBP, stripping with H_2SO_4 solution, precipitation of ammonium metavanadate and calcination. The vanadium recovery of the whole process was 88%. K_2SO_4 intervention at source weakens the negative impacts of Al and Fe ions on solvent extraction and reduces the impurity load of vanadium extraction.

Acknowledgements: This study was funded by the National Natural Science Foundation of China (No. 51404174 and No. 51474162) and the Project in the National Science & Technology Pillar Programme of China (No. 2015BAB18B01).

REFERENCES

- Li J, Zhang YM, Liu T, Huang J, Bao SX (2014) A methodology for assessing cleaner production in the vanadium extraction industry. *J Cleaner Prod* **84**, 598–605.
- Anjum F, Shahid M, Akcil A (2012) Bio-hydrometallurgy techniques of low grade ores: a review on black shale. *Hydrometallurgy* **117–118**, 1–12.
- Zhang YM, Bao SX, Liu T, Chen TJ, Huang J (2011) The technology of extracting vanadium from stone

- coal in China: history, current status and future prospects. *Hydrometallurgy* **109**, 116–24.
4. Zhu XB, Zhang YM, Huang J, Liu T, Wang Y (2012) A kinetics study of multi-stage counter-current circulation acid leaching of vanadium from stone coal. *Int J Miner Process* **114–117**, 1–6.
 5. Wang F, Zhang YM, Liu T, Huang J, Zhao J, Zhang GB, Liu J (2014) Comparison of direct acid leaching process and blank roasting acid leaching process in extracting vanadium from stone coal. *Int J Miner Process* **128**, 40–7.
 6. Yuan YZ, Zhang YM, Liu T, Chen TJ (2015) Comparison of the mechanisms of microwave roasting and conventional roasting and of their effects on vanadium extraction from stone coal. *Int J Miner Metall Mater* **22**, 476–82.
 7. Wang F, Zhang YM, Liu T, Huang J, Zhao J, Zhang GB, Liu J (2015) A mechanism of calcium fluoride-enhanced vanadium leaching from stone coal. *Int J Miner Process* **145**, 87–93.
 8. Li MT, Wei C, Fan G, Li CX, Deng ZG, Li XB (2010) Pressure acid leaching of black shale for extraction of vanadium. *Trans Nonferr Met Soc China* **20**, s112–7.
 9. Barik SP, Park KH, Nam CW (2014) Process development for recovery of vanadium and nickel from an industrial solid waste by a leaching-solvent extraction technique. *J Environ Manag* **146**, 22–8.
 10. Noori M, Rashchi F, Babakhani A, Vahidi E (2014) Selective recovery and separation of nickel and vanadium in sulfate media using mixtures of D2EHPA and Cyanex 272. *Separ Purif Tech* **136**, 265–73.
 11. Nguyen T, Lee MS (2015) Solvent extraction of vanadium(V) from sulfate solutions using LIX 63 and PC 88A. *J Ind Eng Chem* **31**, 118–23.
 12. Nguyen TH, Lee MS (2014) Recovery of molybdenum and vanadium with high purity from sulfuric acid leach solution of spent hydrosulfurization catalysts by ion exchange. *Hydrometallurgy* **147–148**, 142–7.
 13. Nguyen TH, Lee MS (2013) Separation of molybdenum and vanadium from acid solutions by ion exchange. *Hydrometallurgy* **136**, 65–70.
 14. Hu J, Wang XW, Xiao LS (2009) Removal of vanadium from molybdate solution by ion exchange. *Hydrometallurgy* **95**, 203–6.
 15. Huang JW, Su P, Wu WW, Liao S, Qin HQ, Wu XH, et al (2010) Concentration and separation of vanadium from alkaline media by strong alkaline anion-exchange resin 717. *Rare Met* **5**, 439–43.
 16. Wang XW, Wang MY, Shi LH (2010) Recovery of vanadium during ammonium molybdate production using ion exchange. *Hydrometallurgy* **104**, 317–21.
 17. Hu G, Chen D, Wang L, Liu J, Zhao H, Liu Y, et al (2014) Extraction of vanadium from chloride solution with high concentration of iron by solvent extraction using D2EHPA. *Separ Purif Tech* **125**, 59–65.
 18. Li XB, Wei C, Wu J, Li CX, Li MT, Deng ZG, Xu HS (2012) Thermodynamics and mechanism of vanadium(IV) extraction from sulphate medium with D2EHPA, EHEHPA and CYANEX 272 in kerosene. *Trans Nonferr Met Soc China* **22**, 461–6.
 19. Zeng L, Cheng C (2010) Recovery of molybdenum and vanadium from synthetic sulphuric acid leach solutions of spent hydride sulphurisation catalysts using solvent extraction. *Hydrometallurgy* **101**, 141–7.
 20. Tavakoli MR, Dreisinger DB (2014) Separation of vanadium from iron by solvent extraction using acidic and neutral organophosphorus extractants. *Hydrometallurgy* **141**, 17–23.
 21. Kim H, Lee K, Mishra D (2014) Separation and recovery of vanadium from leached solution of spent residue hydro-desulfurization (RHDS) catalyst using solvent extraction. *J Ind Eng Chem* **20**, 4457–62.
 22. Li W, Zhang YM, Liu T, Huang J, Wang Y (2013) Comparison of ion exchange and solvent extraction in recovering vanadium from sulfuric acid leach solutions of stone coal. *Hydrometallurgy* **131–132**, 1–7.
 23. Bao SX, Zhang YM, Huang J, Yang X, Hu YJ (2011) Determination of vanadium valency in roasted stone coal by separate dissolve-potentiometric titration method. In: *Materials Research for Mining and Mineral Processing*, Material Research Society Symposium Proceedings vol 1380, pp 98–103.
 24. Li XB, Wei C, Deng ZG, Li MT, Li CX, Fan G (2011) Selective solvent extraction of vanadium over iron from a stone coal/black shale acid leach solution by D2EHPA/TBP. *Hydrometallurgy* **105**, 359–63.
 25. Zhang HB (1992) *Chemical Phase Analyses of Ores and Industry Products*, 1st edn, Metallurgical Industry Press, Beijing, China, pp 230–50.
 26. Bai L, Peng JH, Zhang JX, Wan TZ (2008) Study on hydration and hardening of natural anhydrite. *Non Met Mines* **31(4)**, 1–3, [in Chinese].
 27. Azimi G, Papangelakis VG (2010) The solubility of gypsum and anhydrite in simulated laterite pressure acid leach solutions up to 250 °C. *Hydrometallurgy* **102**, 1–13.
 28. Gao J, Zhao GY (2013) Experimental research on mechanical properties of recrystallized solid of phosphogypsum. *Min Met Eng* **33(2)**, 18–26, [in Chinese].
 29. Kügler RT, Beißert K, Kind M (2016) On heterogeneous nucleation during the precipitation of barium sulfate. *Chem Eng Res Des* **114**, 30–8.
 30. Heduit A, Thevenot DR (1989) Relation between redox potential and oxygen levels in activated-sludge reactors. *Water Sci Tech* **21**, 947–56.
 31. Wen L, Liang WX, Zhang ZG, Huang JC (1988) *The Infrared Spectroscopy of Minerals*, Chongqing Univ Press, Chongqing, China, pp 98–117.
 32. Crundwell FK (2014) The mechanism of dissolution of minerals in acidic and alkaline solutions: Part II Application of a new theory to silicates, aluminosilicates and quartz. *Hydrometallurgy* **149**, 265–75.